

CERRIC AMMONIUM NITRATE CATALYZED ECO-FRIENDLY GREEN SYNTHESIS OF CHITOSAN SCHIFF BASE USING PEG-400 AS AN ANTICANCER AGENT AGAINST GASTRIC CANCER CELLS VIA INHIBITING EGFR

Wei Geng^{1#}, Xinwei Feng^{2#}, Chunfeng Li³ and Sifeng Ni^{4*}

¹VIP Health Management Center, Xi'an International Medical Center Hospital, Xi'an, Shaanxi, 710100, China

²Department of Digestive Internal Medicine, Shanghai Changzheng Hospital Shanghai 200003, China

³Department of Gastrointestinal Surgical Ward, Harbin Medical University Cancer Hospital, Harbin, 150081, China

⁴Department of Nursing, Xi'an International Medical Center Hospital, Xi'an, Shaanxi, 710100, China

(Received January 15, 2024; Revised March 5, 2024; Accepted March 10, 2024)

ABSTRACT. The present study was conducted to scrutinize the pharmacological effect of oxazole-embedded Chitosan as an anticancer agent against gastric cancer cells. This compound was synthesized using the classical Schiff base reaction but utilizing the novel green chemical process where ceric ammonium nitrate (CAN) was used as a catalyst in the PEG-400 as solvent media. The target compound was obtained with an excellent yield at the catalyst loading of 5% CAN concentration in 15 min. The Kinase-Glo Plus luminescence kinase assay kit was used to determine the EGFR inhibitory activity of compound **1** where it showed potent activity with IC₅₀ of 2.14 μM. Its effect was also determined on the cellular viability of the Human gastric cancer cell line (SGC7901), liver cancer cell line (HepG2), and lung cancer cell line (A549), where it exhibits potent activity against SGC7901. The compound further showed the concentration-dependent inhibitory effect on migration and invasion of SGC7901. In RT-qPCR analysis, the compound showed induction of apoptosis of SGC7901 cells possibly by restoring the expression of Bcl-2 and Bax near to normal, and inhibition of the mRNA expression of EGFR in a concentration-dependent manner.

KEY WORDS: Schiff base; Chitosan; EGFR, mRNA, apoptosis, Bcl-2

INTRODUCTION

Gastric cancer is the fourth leading cause of cancer and is responsible for 769,000 deaths and one million new cases that occur annually [1]. The clinical outcomes that are achieved through the use of various therapeutic options for gastric cancer, such as radiation therapy, chemotherapy, and surgical excision, are not always favorable. In most cases, the discovery of gastric cancer occurs after the disease has already spread to other areas of the body which leads to the poor prognosis of the disease [2, 3]. It is of the utmost importance to develop novel or improved combination chemotherapy regimens to improve the outcome for individuals suffering from stomach cancer and to combat resistance to drugs.

Chitosan, a naturally occurring biopolymer, can be generated from chitin by either enzymatic or chemical processes at high temperatures [4]. Because of its high bioavailability, drug-carrier capacity, and ease of penetration across the cell membrane, it was a promising scaffold for the delivery of drugs for the identification of new drugs [5]. According to the findings of several research, it possesses remarkable anti-cancer, antibacterial, and antioxidant effects [6, 7]. Furthermore, it has been discovered that the production of Schiff bases, which mostly took place

*Corresponding authors. E-mail: haohjnsf@sina.com

#Wei Geng and Xinwei Feng are co-first authors, they contributed equally to this work.

This work is licensed under the Creative Commons Attribution 4.0 International License

as a consequence of the azomethine link, has significantly contributed to the enhancement of the pharmacological activity of chitosan [8, 9]. Studies showed that Schiff bases are the condensation products of primary amines with carbonyl compounds, and endowed with a variety of pharmacological activity. It showed excellent anticancer, antibacterial, anti-inflammatory, anti-convulsant, and anthelmintic activity [10].

Oxazole is another vital pharmacophore responsible for a diverse array of pharmacological activity, such as anti-fungal, antibacterial, antimalarial, and anticancer activity [11, 12]. Various clinically available molecules, such as linezolid, furazolidone, toloxatone, oxaprozin, ditazole, and aleglitazar contain oxazole as a core scaffold [13].

Therefore, the present study was conducted to analyze the anticancer effect of oxazole-embedded chitosan Schiff base (OCS) against gastric cancer cells and their mechanism of action.

EXPERIMENTAL

Chemical and reagents

All the chemicals and reagents used in the present study were procured from Sigma Aldrich (USA) without further purification unless otherwise stated. ^1H NMR spectra were recorded in *d*₆-DMSO on a Bruker Avance-400 NMR spectrometer with TMS as the internal reference. ^{13}C NMR spectra were recorded on a Bruker Avance-100 NMR spectrometer in *d*₆-DMSO on the same spectrometers with TMS as the internal reference. The multiplicity of a signal is indicated as: s – singlet, d – doublet, t – triplet, q – quartet, m – multiplet, br – broad, dd – doublet of doublets, etc. Coupling constants (*J*) are quoted in Hz and reported to the nearest 0.1 Hz. Infrared spectra were recorded as a neat thin film on a Perkin-Elmer Spectrum One FT-IR spectrometer using Universal ATR sampling accessories. Melting points were obtained using MEL-TEMP (model 1001D).

General procedure for the synthesis of pyrazole-based Schiff bases of Chitosan

PEG-400 was used as the solvent for the reaction of chitosan (1 mmol) and the corresponding oxazole 4-carbaldehyde (1 mmol). After adding CAN at a concentration of 5% to the previous mixture and stirring it for 20 min while it was heated to 80 °C, the desired end product (**1**) was obtained. TLC was utilized to track both the progression and conclusion of the reaction mixture. After the reaction was finished, the mixture that had been obtained above was chilled in acetone and a dry ice bath to precipitate the PEG-400, and then it was extracted using ether because PEG-400 is insoluble in ether. After being decanted, the ether layer was allowed to dry and then concentrated while the pressure was lowered. Various spectral analysis was performed to determine the structures of all of the product, and these data were found in agreement with the previous study [14].

Oxazole-embedded Chitosan Schiff base

Yield: 79%; *R*_f: 0.72; FTIR (ν_{max} ; cm^{-1} , in KBr): 3592 (OH stretching), 3024 (aromatic C-H stretching), 2947 (CH_2 stretching), 1678 (C=N stretching), 1522 (C=C stretching), 1269 (C-O stretching), 1228 (C-N stretching), 1173 (C-O-C stretching), 751; ^1H NMR (400 MHz, DMSO-*d*₆, TMS) δ ppm: 8.13 (s, 1H, C-H), 8.11 (d, 1H, *J* = 1.35 Hz, Oxazol-H), 7.91 (d, 1H, *J* = 1.32 Hz, Oxazol-H), 5.06 (d, 1H, *J* = 2.91 Hz, Chitosan-H), 4.51-4.32 (m, 3H, 3×OH Chitosan) 3.94 (s, 1H, $\text{CH}_2\text{-O-H}$), 3.79 (d, 2H, *J* = 7.98 Hz, Chitosan- CH_2), 3.73 (d, 1H, *J* = 2.18 Hz, Chitosan-H), 3.51 (d, 1H, *J* = 7.98 Hz, Chitosan-H), 3.31 (d, 1H, *J* = 2.14 Hz, Chitosan-H), 3.18 (d, 1H, *J* = 3.48 Hz, Chitosan-H), 1.51 (d, 1H, *J* = 3.62 Hz, Chitosan-H); ^{13}C NMR (100 MHz, DMSO-*d*₆) δ ppm: 154.8, 151.4, 141.5, 125.7, 96.8, 81.1, 73.2, 72.8, 71.9, 62.3.

Cell culture

Human gastric cancer cell line (SGC7901), liver cancer cell line (HepG2), and lung cancer cell line (A549) were obtained from the American Type Culture Collection (ATCC, USA) and cultured as per the instructed protocol [15]. The cells were cultured in Dulbecco's Modification of Eagle's Medium (DMEM) (Cellgro, Manassas, VA, USA), supplemented with 10% fetal bovine serum (FBS), 1% penicillin/streptomycin (Invitrogen Co.) and 4mM *L*-glutamine in an atmosphere of 5% CO₂ at 37 °C.

EGFR Kinase inhibition assay

EGFR Kinase inhibitory activity was determined using a ADP-Glo™ kinase detection kit. It is a luminescence kinase detection approach that detects the amount of ADP produced by the kinase reaction. After ADP is converted into ATP, ATP can be used as the substrate of the luciferase-catalyzed reaction to generate an optical signal, which is positively correlated with kinase activity. An ADP-Glo™ kinase detection kit can detect the activities of almost all enzymes that can produce ADP, and the concentration of ATP can be as high as 1 mmol. The target compound **1** were formulated into solutions of different concentrations, and three independent experiments were performed for each group. The following components were added to the 384-well plate: 5 µL of kinase buffer containing 20 µmol ATP and 2 µmol PIP2 (25 mmol 3-morpholinopropanesulfonic acid, 12.5 mmol β-glycerophosphoric acid, 5 mmol EGTA, 2 mmol EDTA, and 0.25 mmol DTT); 2 µL (50 ng/mL) of EGFR kinase; and 2.5 µL of dimethyl sulfoxide solution containing different concentrations of the test compound. The above-prepared systems were sealed and incubated at room temperature for 2 h, and 5 µL of ADP-GLO was added to terminate the kinase reaction. Then, the culture plate was sealed and incubated in a thermostatic oscillator for 40 min to fully consume the remaining ATP. The luciferase/luciferin reaction was adopted to determine the newly generated ATP level. The signals of ADP/ATP varied according to the inhibitory effects of the target compound, the luminescence values of each well were measured with plate counter, and the data were further converted into IC₅₀ values [15].

Treatment group

Various treatment groups have been formed based on a diverse range of concentration of compound as follows: Group 1: 0 µM; Group 2: 2.5 µM; Group 3: 5 µM; Group 4: 10 µM.

Cell proliferation assay

Using the MTT assay, which involves the use of RPMI1640 or DMEM supplemented with 10% fetal bovine serum (HyClone) and 1% penicillin-streptomycin liquid (Gibco), cell proliferation was evaluated. Chemicals or the control solvent were then added to the panel of cells at varying concentrations. The experiment continued for another four hours at 37 °C after the first 48 hours of incubation, during which 2.5 mg mL⁻¹ of MTT reagent was added. Microplate readers (PerkinElmer, Enspire 2300, USA) were used to detect absorbance at 490 nm. The GraphPad Prism was used to plot dose-response curves, which allowed the IC₅₀ values to be ascertained [15].

Wound healing assay

After seeding SGC7901 cells onto 12-well culture dishes, they were manually scratched using a 1-mL pipette tip to damage their surface. To eliminate any remaining cell debris, the scratched surface was rinsed with PBS. After that, the cells were placed on dishes and incubated at 37 °C

for 48 hours after being treated with the compound-containing medium. Additionally, seed the cells at a density of 3×10^5 /mL. The compound **1** was left to incubate with the cells for an extra 48 hours at 37 °C. At 0 hours (control) and 48 hours, an inverted microscope with a total magnification of 40× was used to take images of the wound sites. The area of each wound was measured using the ImageJ program.

Invasion assay

The upper transwell inserts (Corning Inc., Cat#. 354480) were seeded with SGC7901 cells (1×10^5 cells) that had been suspended in serum-free media containing the compound **1**. A 20% FBS-containing medium was added to the bottom chambers. Transwell inserts were incubated for 30 hours before being preserved with cold methanol and stained with 0.5% Crystal Violet. With an inverted microscope set at 100× total magnification, the non-invaded cells were removed and the invaded cells were counted in four fields that were chosen at random.

RT-qPCR analysis

We followed the manufacturer-provided instructions to extract total RNA using a Total RNA Isolation Kit (RC101-01, Vazyme). The NanoDrop 2000, made by Thermo Fisher Scientific, was used to measure the total RNA. The procedure included the use of the HiScript® III All-in-one RT SuperMix (R333-01, Vazyme) to transform total RNA into complementary DNA (cDNA). One step real-time RT-PCR was performed using the ChamQ SYBR Color qPCR Master Mix (Q411-02, Vazyme). The Δ CT approach was used to ascertain the target gene's gene expression levels.

Table 1. Sequence of primers used for RT-PCR analysis.

Genes	Sequence (5'-3')
B-actin	F: CATTGCTGACAGGATGCAGA
	R: CTGCTGGAAGGTGGACAGTGA
Bcl-2	F: GAGGATTGTGGCCTTCTTG
	R: AGGTAAGTCAATCCACA
Bax	F: ATGGAGCTGCAGAGGATGA
	R: CCAGTTTGCTAGCAAAGTAG
EGFR	F: GCCATCTGGGCCAAAGATACC
	R: GTCTTCGCATGAATAGGCCAAT

Statistical analysis

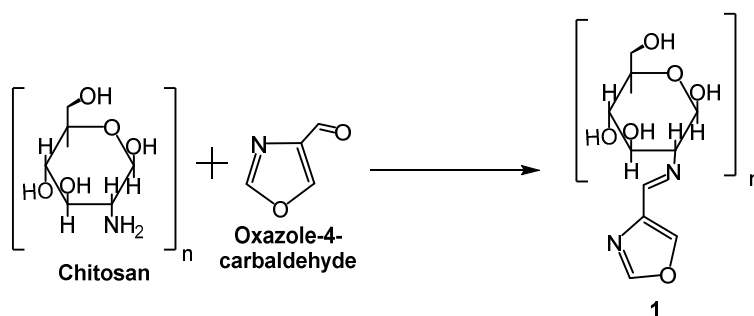
Statistical analysis was conducted using the GraphPad Prism software (v.8.0). There was a minimum of three repetitions of each in vitro experiment. A two-tailed Student's t-test was used to assess the variations between the two groups. We compared the differences across several groups using analysis of variance and expressed as mean \pm SEM. $p < 0.05$ was considered to be statistically significant.

RESULTS AND DISCUSSION

Chemistry

The synthesis of oxazole-embedded chitosan Schiff base was achieved using the CAN as a catalyst in PEG-400 and has been shown in Scheme 1. The reaction mixture consists of an equimolar quantity of carbonyl compound (oxazole) and chitosan in PEG-400 using catalyst

loading of 5% CAN at 80 °C. It was found that the reaction was completed in 15 min to afford the desired target compound with an 83% yield. FT-IR, ^1H NMR, and ^{13}C NMR spectroscopy techniques were employed to verify the structure of synthesized compound **1**. In FT-IR spectra, a distinctive band corresponding to C-H in the oxazole ring was appeared at 3024 cm^{-1} . The strong band at 3592 cm^{-1} is due to OH stretching. A prominent band of the CH_2 group in the chitosan ring was observed at 2947 cm^{-1} . The stretching vibration of the C=N group linked to the oxazole ring was observed at 1678 cm^{-1} . The stretching vibration of the C=C group was observed at 1522 cm^{-1} . A strong bond at 1269 cm^{-1} is attributed to C-O stretching. The ^1H NMR spectral analysis was also conducted where the doublet peak at 8.11-7.91 ppm attributed to the aromatic oxazole ring proton. An additional doublet peak was also observed at 5.06 ppm due to the aliphatic CH proton group of the Chitosan-H ring. Multiple peaks of the Chitosan-H ring connected with the oxazole ring proton were seen between 4.51-4.32 ppm. The chitosan exhibited a singlet peak at 3.94 ppm. Moreover, doublet peak of Chitosan-H ring aliphatic proton were observed at 3.79-1.51 ppm. The title compounds exhibited resonance peaks ranging from 151.4 to 125.7 ppm attributed to carbon atoms in the oxazole ring. The side chain carbon atoms are linked to the oxazole ring appeared at 154.8 ppm. The aliphatic carbon atoms of the chitosan connection with oxazole ring were observed at 96.8-62.3 ppm.



Scheme 1. Synthesis of oxazole-embedded-Chitosan Schiff base. Reagents and condition: 5% CAN, PEG-400, 80 °C.

Pharmacological activity

The EGFR kinase plays a crucial role in the survival and progression of several malignancies, including gastric cancer (GC) [16]. By inhibiting the function of apoptosis-related genes such as BAD, BAX, caspase-9, and GSK-3, it plays a critical role in promoting the survival of cancer cells [17]. This ultimately leads to increased cell viability, enhanced potential to spread to other parts of the body, formation of new blood vessels, and resistance to chemotherapy. It enhances the presence of chemicals that prevent cell death, such as NF- κ B, cAMP, and CREB, leading to a greater ability to develop, spread to other parts of the body, and resist treatment [18]. As a result, researchers are dedicating a substantial amount of their attention to studying and finding drugs that block the EGFR signaling pathway, and new therapies are constantly being developed. In the present study, the compound was tested for EGFR inhibitory activity using ELISA-based Kinase Glo Enzyme assay. As presented in Table 2, it showed potent inhibition of EGFR with IC_{50} of 2.14 μM .

Table 2. Inhibitory effect of compound **1** on the EGFR kinase.

Code	EGFR Kinase inhibition (IC ₅₀ , in μM) ^a
1	2.14 \pm 0.76 μM

Where ^a denotes the Mean \pm SEM of three replicates.

Cell viability assay

The effect of the compound-**1** was investigated on the cellular viability of various human cancer cells, such as the human gastric cancer cell line (SGC7901), liver cancer cell line (HepG2), and lung cancer cell line (A549). As shown in Table 3, compound **1** showed least activity against A549 cells with IC₅₀ of 124.64 \pm 10.32 μM and moderate activity against Hep G2 cells with IC₅₀ of 47.24 μM . The most potent activity was reported against the gastric cancer cells with 7.45 \pm 0.84 μM . Therefore, subsequent investigations were conducted to study the mechanism of the anticancer action of compound **1** utilizing SGC7901 cells with the help of several biochemical assays.

Table 3. Effect of compound **1** on the cellular viability of various human cancer cells.

Code	IC ₅₀ (in μM) ^a		
	SGC7901	HepG2 (liver)	A549 (lung)
1	7.45 \pm 0.84	47.24 \pm 2.53	124.64 \pm 10.32

Where ^a denotes the Mean \pm SEM of three replicates.

Apoptosis and cell-cycle arrest of SGC7901 cells

Various studies suggest that many clinically available anticancer drugs induce apoptosis by causing cell-cycle arrest [19]. Apoptosis is considered a vital biological process of cellular death that is intended to happen without the release of internal cellular components, therefore preventing the initiation of an inflammatory reaction [20]. It is regarded as a vital mechanism in the development of embryos, the control of the immune system, and the reaction to DNA damage. Nevertheless, the disruption of apoptosis leads to a prolonged period for the build-up of genetic alterations, which can heighten the ability of tumors to spread, trigger the formation of new blood vessels, disrupt the control of cell growth, and impede the process of cellular specialization [21]. Moreover, the cell cycle is a sequence of closely interconnected processes that enable the cell to expand and reproduce. These processes allow the cell to grow and reproduce. Furthermore, cell cycle arrest is a crucial mechanism that has been demonstrated to contribute to the anticancer effects of a wide variety of well-established drugs. By selectively targeting proteins, certain anticancer drugs are able to block the passage of cells from one phase of the cell cycle to another. This, in turn, causes an accumulation of cancer cells at a certain stage. It is also possible for the cell cycle arrest to restrict the multiplication of cancer cells as well as their ability to spread to distant organs [22]. Therefore, in the next part, we aimed to scrutinize the pharmacological effect of compound **1** on the apoptosis and cell-cycle of SGC-7901 cells. As shown in Figure 1a, compound **1** causes concentration-dependent induction of apoptosis of SGC-7901 cells as compared to non-treated control. Moreover, our study has also revealed that Compound **1** can increase the number of cells in the G2/M phase while decreasing the number of cells in the S-phase. Additionally, no significant change in the G0/G1 cell population was observed in any of the groups. One possible explanation for compound **1**'s potent anti-proliferative effects on SGC-7901 cells is via targeting cell cycle progression at the G2/M phase and stimulating apoptosis.

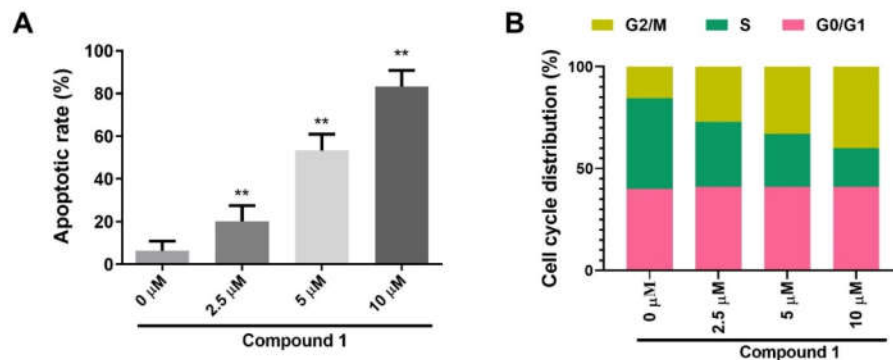


Figure 1. Effect of compound 1 on the apoptotic rate and cell-cycle distribution of SGC-7901 cells. Data presented as mean \pm SEM (n = 3). ** $p < 0.05$ vs. non-treated group.

Migration and invasion of SGC-7901 cells

Patients' chances of survival are greatly affected by the order in which tumor cell invasion and metastasis progress. Metastasis is a process by which primary malignancies in one organ can spread to other organs. In particular, this mechanism is to blame for cancer's devastating toll on human health [23]. When tumor cells acquire the ability to invade neighbouring tissues, they do so by penetrating the basement membrane and extracellular matrix. As the cells enter the lymphatic or vascular circulation, this process culminates in intravasation. Metastatic cells then invade the vascular basement membrane and extracellular matrix as they travel through the bloodstream, a process known as extravasation [24, 25]. Ultimately, the secondary tumor will be formed when these cells adhere to a new location and proliferate which ultimately results in poor prognosis. Thus, in the next study, we aimed to analyze the effect of compound 1 on the migration and invasion ability of SGC7901 cells. As shown in Figure 2, compound 1 causes significant reduction both migration invasion of SGC7901 cells in the concentration dependent manner.

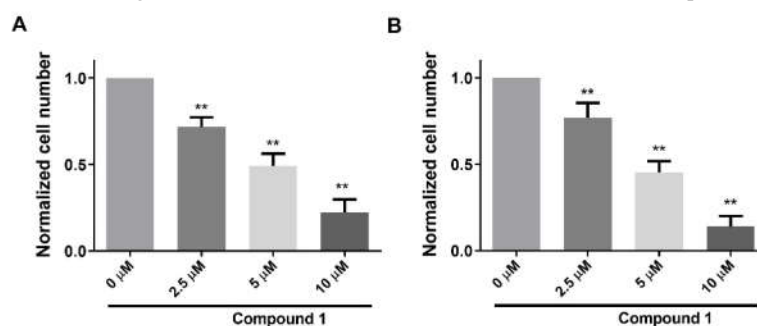


Figure 2. Effect of compound 1 on the (A) migration and (B) invasion of SGC-7901 cells. Data presented as mean \pm SEM (n = 3). ** $p < 0.05$ vs. non-treated group.

Expression of Bax and Bcl2 using RT-PCR in SGC-7901 cells

The regulation of cellular apoptosis by Bax and Bcl-2 is crucial for tissue homeostasis. Bax triggers cell death by releasing substances that promote cell death through openings in the

mitochondrial outer membrane [26]. On the other hand, Bcl-2 is a protein that stops cells from dying by keeping mitochondria intact and preventing Bax. Apoptosis is facilitated by an excess of Bax and inhibited by an excess of Bcl-2; the cellular fate is dictated by this equilibrium [27]. Many diseases, including cancer, are linked to an imbalance in this equilibrium, which causes a fall in Bax levels and an increase in Bcl-2, which promotes cell survival and inhibits cell death. Numerous anti-cancer treatments induce apoptosis by elevating the level of Bax while simultaneously decreasing the level of Bcl-2 [28]. During this investigation, as illustrated in Figure 3, compound **1** showed a noteworthy rise in the expression of Bax, while simultaneously exhibiting a decline in the level of Bcl-2. Thus, it could be suggested that compound **1** induces apoptosis via restoring the level of Bax and Bcl2.

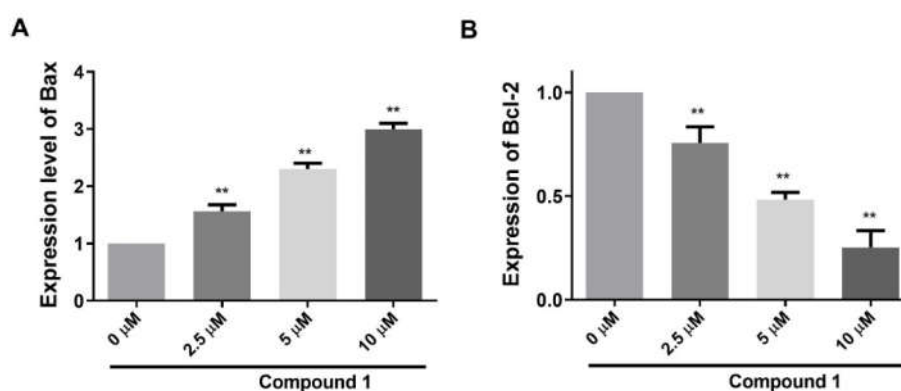


Figure 3. Effect of compound **1** on expression of (a) Bax and (b) Bcl-2 using RT-PCR in SGC7901 cells. Data presented as mean \pm SEM (n = 3). ** $p < 0.05$ vs. non-treated group.

Expression of EGFR in SGC-7901 cells using RT-PCR

As a transmembrane receptor tyrosine kinase, EGFR is expressed in certain normal neurogenic, mesenchymal, and epithelial tissues [29]. There have been reports of EGFR overexpression and its potential role in the development of many human cancers, including NSCLC [30]. Evidence suggests that EGFR expression in NSCLC is linked to worse chemosensitivity, shorter survival times, and more lymph node metastases [31]. Patients with advanced NSCLC are commonly treated with chemotherapy, while those with early-stage NSCLC typically undergo surgical resection. Patients with non-small cell lung cancer (NSCLC) who have corresponding genetic alterations are often prescribed molecular targeted therapy regimens [32]. Priority is given to patients who have EGFR-sensitizing mutations, such as EGFR exon 19 deletion (Ex19del) or L858R mutations, which are inhibitors of epidermal growth factor receptor tyrosine kinase. To treat patients with non-small cell lung cancer (NSCLC) who have EGFR mutations, three separate generations of EGFR-TKIs have been approved for use in various clinical contexts. Gefitinib, erlotinib, and icotinib are first-generation drugs; afatinib and dacomitinib are second-generation drugs. Patients with advanced non-small cell lung cancer (NSCLC) with mutations Ex19del and L858R have shown significant clinical improvement after using EGFR-TKIs [33]. Many patients will acquire resistance to EGFR-TKIs within 9 to 14 months of starting or continuing treatment with these drugs, even though first- and second-generation EGFR-TKIs have strong initial effects. Therefore, new chemical development to suppress EGFR and enhance gastric cancer prognoses is an urgent necessity. Thus, in the present study, we have determined the effect of compound **1** on the mRNA expression of EGFR. Our result showed that compound **1** causes significant

reduction in the expression of EGFR as compared to non-treated control in a concentration concentration-dependent manner. The most prominent inhibition was observed in the 10 μM treated group as compared to untreated group.

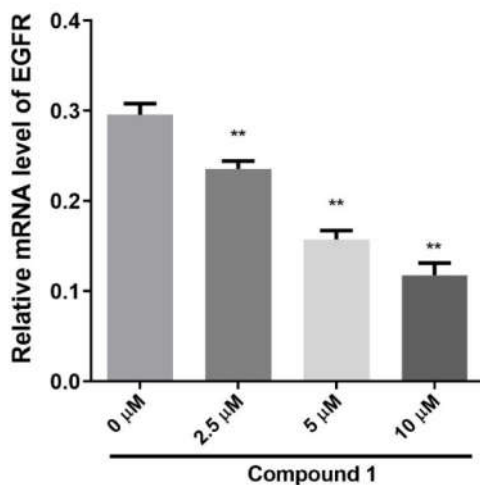


Figure 4. Effect of compound **1** on the expression of EGFR in SGC7901 cells. Data presented as mean \pm SEM (n = 3). ** $p < 0.05$ vs. non-treated group.

CONCLUSION

In conclusion, our study showed the development of eco-friendly green synthesis of oxazole-embedded chitosan Schiff base (compound **1**) using 5% CAN as catalyst in PEG-400. The in-vitro studies suggest that compound **1**, induces apoptosis, inhibition of cell-migration and invasion, and mRNA expression of EGFR in SGC7901 cells. It also showed G2/M phase cell cycle arrest with induction of Bax, and inhibition of Bcl-2 levels. We concluded that the EGFR signalling pathway might exert a significant effect on compound **1** mediated anti-cancerous effects in gastric cancer cells. The study does not have in-vivo outcomes. It is essential to apply the results of this study to animal models to demonstrate the effects obtained from the in vitro experiments.

REFERENCES

1. Necula, L.; Matei, L.; Dragu, D.; Neagu, A.I.; Mambet, C.; Nedecianu, S.; Bleotu, C.; Diaconu, C.C.; Chivu-Economescu M. Recent advances in gastric cancer early diagnosis. *World J. Gastroenterol.* **2019**, *25*, 2029-2044.
2. He, Y.; Wang, Y.; Luan, F.; Yu, Z.; Feng, H.; Chen, B.; Chen, W. Chinese and global burdens of gastric cancer from 1990 to 2019. *Cancer Med.* **2021**, *10*, 3461-3473.
3. Wang, S.M.; Zheng, R.S.; Zhang, S.W.; Zeng, H.M.; Chen, R.; Sun, K.X.; Gu, X.Y.; Wei, W.W.; He, J. Epidemiological characteristics of gastric cancer in China, 2015. *Zhonghua Liu Xing Bing Xue Za Zhi* **2019**, *40*, 1517-1521.
4. Aranaz, I., Alcántara, A.R., Civera, M.C., Arias, C., Elorza, B., Heras Caballero, A.; Acosta, N. Chitosan: An overview of its properties and applications. *Polymers* **2021**, *13*, 3256.

5. Parhi R. Drug delivery applications of chitin and chitosan: a review. *Environ. Chem. Lett.* **2020**, 18, 577-594.
6. Kumar, M.N.V.R.; Muzzarelli, R.A.A.; Muzzarelli, C.; Sashiwa, H.; Domb, A.J.; Chitosan chemistry and pharmaceutical perspectives. *Chem. Rev.* **2004**, 104, 6017-6084.
7. Kou, S.G.; Peters, L.; Mucalo, M. Chitosan: A review of molecular structure, bioactivities and interactions with the human body and micro-organisms. *Carbohydr. Polym.* **2022**, 282, 119132
8. Wei, L.; Zhang, J.; Tan, W.; Wang, G.; Li, Q.; Dong, F.; Guo, Z. Antifungal activity of double Schiff bases of chitosan derivatives bearing active halogeno-benzenes. *Int. J. Biol. Macromol.* **2021**, 179, 292-298.
9. Packialakshmi, P.; Gobinath P.; Ali, D.; Alarifi, S.; Gurusamy, R.; Idhayadhulla, A.; Surendrakumar, R. New Chitosan polymer Scaffold Schiff bases as potential cytotoxic activity: Synthesis, molecular docking, and physiochemical characterization. *Front. Chem.* **2022**, 9, 796599.
10. Shanty, A.A., Philip, J.E., Sneha, E.J., Prathapachandra Kurup, M.R.; Balachandran, S.; Mohanan, P.V. Synthesis, characterization and biological studies of Schiff bases derived from heterocyclic moiety. *Bioorg. Chem.* **2017**, 70, 67-73.
11. Joshi, S.; Mehra, M.; Singh, R.; Kakar, S. Review on chemistry of oxazole derivatives: Current to future therapeutic prospective. *Egypt. J. Basic Appl. Sci.* **2023**, **10**, 218-239.
12. Kakkar, S.; Narasimhan, B. A comprehensive review on biological activities of oxazole derivatives. *BMC Chem.* **2019**, 13, 16.
13. Kaur, R.; Palta, K.; Kumar, M.; Bhargava, M.; Dahiya, L. Therapeutic potential of oxazole scaffold: a patent review (2006-2017). *Expert Opin. Ther. Pat.* **2018**, 28, 783-812.
14. Haj, N.Q.; Mohammed, M.O.; Mohammood, L.E. Synthesis and biological evaluation of three new Chitosan Schiff base derivatives. *ACS Omega* **2020**, 5, 13948-13954.
15. Srivastava, J.K.; Pillai, G.G.; Bhat, H.R.; Verma, A.; Singh, U.P. Design and discovery of novel monastrol-1,3,5-triazines as potent anti-breast cancer agent via attenuating epidermal growth factor receptor tyrosine kinase. *Sci. Rep.* **2017**, 7, 5851.
16. Paez, J.G.; Jänne, P.A.; Lee, J.C.; Tracy, S.; Greulich, H.; Gabriel, S.; Herman, P.; Kaye, F.J.; Lindeman, N.; Boggon, T.J.; Naoki, K.; Sasaki, H.; Fujii, Y.; Eck, M.J.; Sellers, W.R.; Johnson, B.E.; Meyerson, M. EGFR mutations in lung, cancer: Correlation with clinical response to gefitinib therapy. *Science* **2004**, 304, 1497-500.
17. Khaddour, K.; Jonna, S.; Deneka, A.; Patel, J.D.; Abazeed, M.E.; Golemis, E.; Borghaei, H.; Bumber, Y. Targeting the epidermal growth factor receptor in EGFR-mutated lung cancer: Current and emerging therapies. *Cancers* **2021**, 13, 3164.
18. Zhang, Z.; Stiegler, A.L.; Boggon, T.J.; Kobayashi, S.; Halmos, B. EGFR-mutated lung cancer: a paradigm of molecular oncology. *Oncotarget.* **2010**, 1, 497-514.
19. Elmore, S. Apoptosis: A review of programmed cell death. *Toxicol. Pathol.* **2007**, 35, 495-516.
20. Lowe, S.W.; Lin, A.W. Apoptosis in cancer. *Carcinogenesis* **2000**, 21, 485-495.
21. Fernald, K.; Kurokawa, M. Evading apoptosis in cancer. *Trends Cell Biol.* **2013**, 23, 620-633.
22. Carneiro, B.A.; El-Deiry, W.S. Targeting apoptosis in cancer therapy. *Nat. Rev. Clin. Oncol.* **2020**, 17, 395-417.
23. Kushwaha, P.P.; Gupta, S.; Singh, A.K.; Kumar, S. Emerging role of migration and invasion enhancer 1 (MIEN1) in cancer progression and metastasis. *Front. Oncol.* **2019**, 9, 868.
24. Seba, V.; Silva, G.; Dos Santos, M.B, Baek, S.J.; França, S.C.; Fachin, A.L.; Regasini, L.O.; Marins M. Chalcone derivatives 4'-amino-1-naphthyl-chalcone (D14) and 4'-amino-4-methyl-1-naphthyl-chalcone (D15) suppress migration and invasion of osteosarcoma cells mediated by p53 regulating emt-related genes. *Int. J. Mol. Sci.* **2018**, 19, 2328.
25. Chen, G.; Chen, S.M.; Wang, X.; Ding, X.F.; Ding, J.; Meng, L.H. Inhibition of chemokine (CXC motif) ligand 12/chemokine (CXC motif) receptor 4 axis (CXCL12/CXCR4)-mediated

- cell migration by targeting mammalian target of rapamycin (mTOR) pathway in human gastric carcinoma cells. *J. Biol. Chem.* **2012**, 287, 12132-12141.
26. Dai, H.; Meng, W.; Kaufmann, S. BCL2 family, mitochondrial apoptosis, and beyond. *Cancer Transl. Med.* **2016**, 2, 7.
 27. Zinkel, S.; Gross, A.; Yang, E. BCL2 family in DNA damage and cell cycle control. *Cell Death Diff.* **2006**, 13, 1351-1359.
 28. Korbakis, D.; Scorilas, A. Quantitative expression analysis of the apoptosis-related genes BCL2, BAX and BCL2L12 in gastric adenocarcinoma cells following treatment with the anticancer drugs cisplatin, etoposide and taxol. *Tumour. Biol.* **2012**, 33, 865-875.
 29. Nicholson, R.I.; Gee, J.M.W.; Harper, M.E. EGFR and cancer prognosis. *Eur. J. Cancer* **2001**, 37, 9.
 30. Brand, T.M.; Lida, M.; Luthar, N. Starr, M.M.; Huppert, E.J.; Wheeler, D.L. Nuclear EGFR as a molecular target in cancer. *Radiother. Oncol.* **2013**, 108, 370-377.
 31. Qiao, M.; Jiang, T.; Liu, X.; Mao, S.; Zhou, F.; Li, X.; Zhao, C.; Chen, X.; Su, C.; Ren, S.; Zhou, C. Immune checkpoint inhibitors in EGFR-Mutated NSCLC: Dusk or dawn? *J. Thorac. Oncol.* **2021**, 16, 1267-1288.
 32. Le, X.; Nilsson, M.; Goldman, J.; Reck, M.; Nakagawa, K.; Kato, T.; Ares, L.P.; Fridmott-Moller, B.; Wolff, K.; Visseren-Grul, C.; Heymach, J.V.; Garon, E.B. Dual EGFR-VEGF pathway inhibition: A promising strategy for patients with EGFR-Mutant NSCLC. *J. Thorac. Oncol.* **2021**, 16, 205-215.
 33. Fu, K.; Xie, F.; Wang, F.; Fu, L. Therapeutic strategies for EGFR-mutated non-small cell lung cancer patients with osimertinib resistance. *J. Hematol. Oncol.* **2022**, 15, 173.